

First Scientific Results from AMS-02



Text

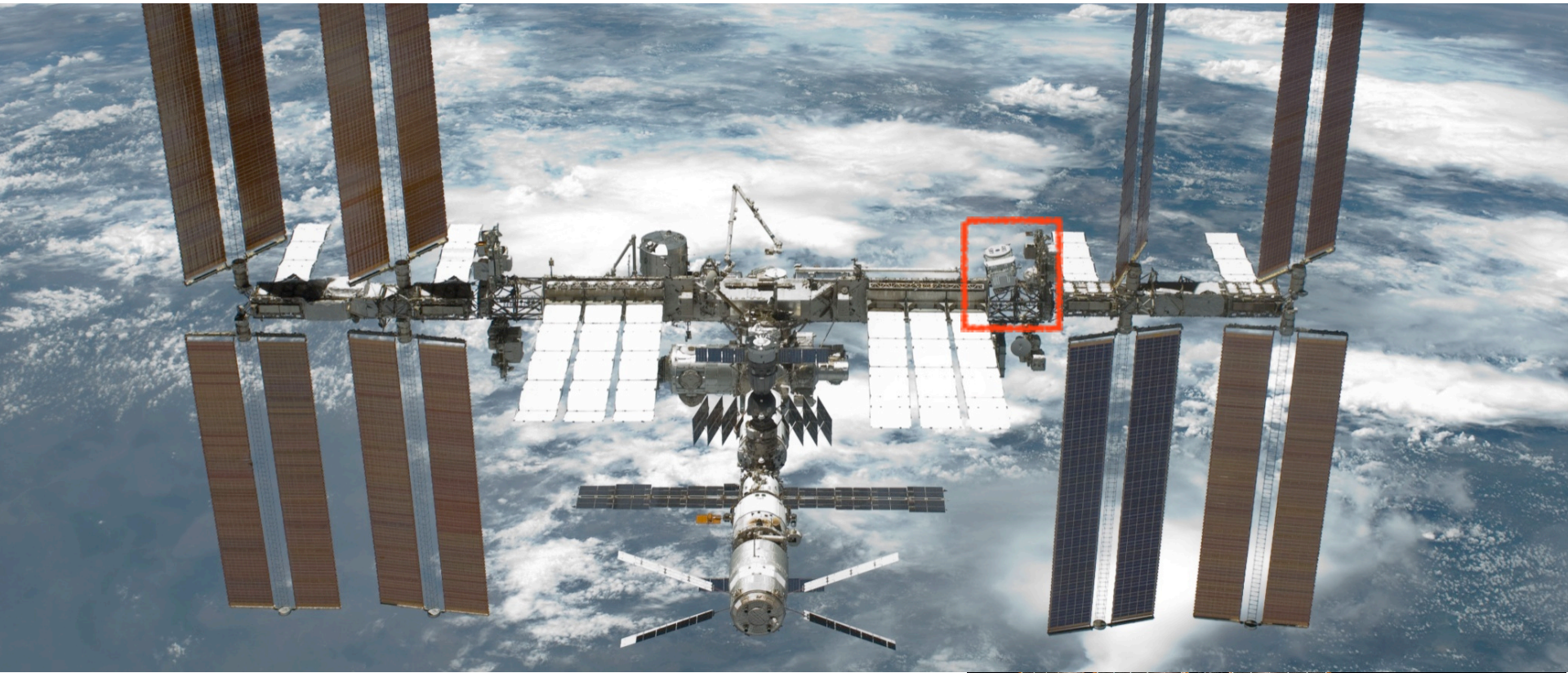
Veronica Bindi

Physics and Astronomy Department University of Hawaii at Manoa



AMS is a US DOE lead International Collaboration

Spokesperson: Nobel laureate Prof. Dr. S. Ting from MIT



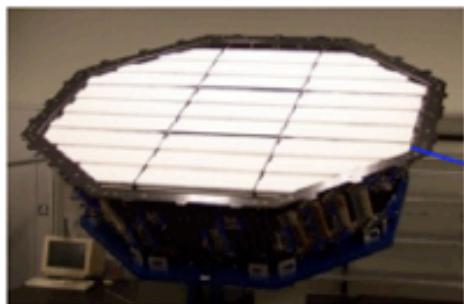
**AMS has been installed on the
International Space Station on
May 19th 2011**



AMS consists of 5 sub-detectors which provide redundant information for particle identification

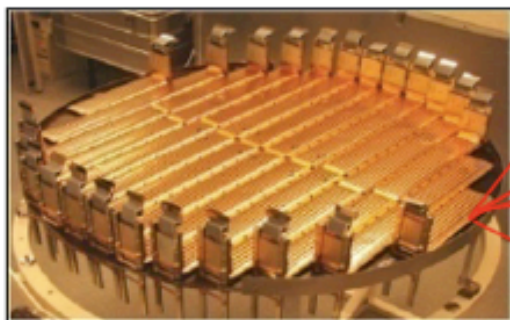
TRD

Identify e^+ , e^-



Silicon Tracker

Z, P

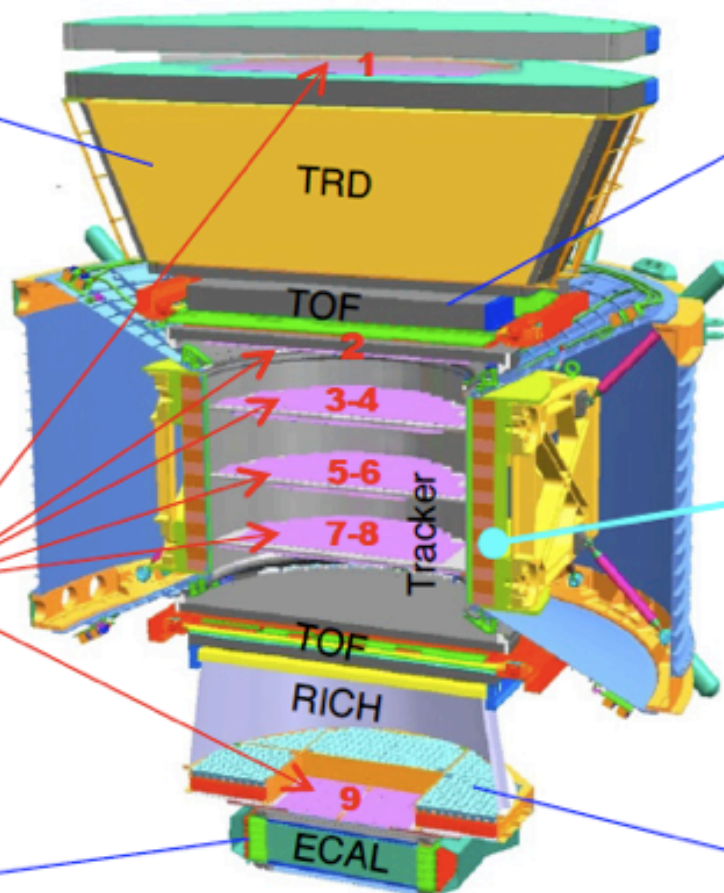


ECAL

E of e^+ , e^- , γ



Particles and nuclei are defined by their charge (Z) and energy ($E \sim P$)



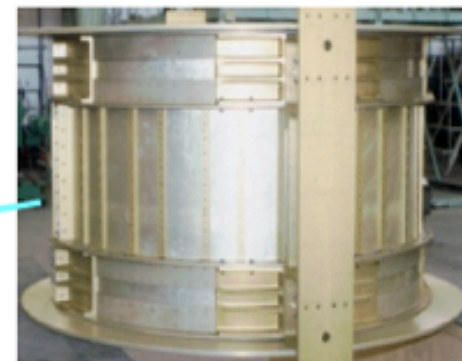
TOF

Z, V



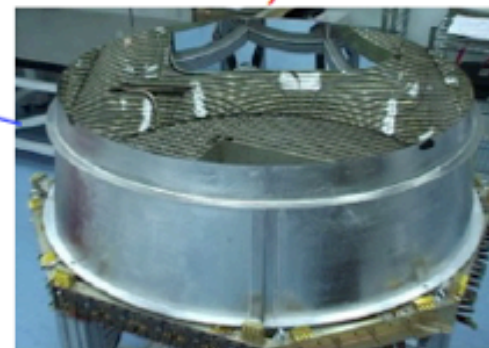
Magnet

$\pm Z$



RICH

Z, V



Scientific goals of AMS on the International Space Station

Indirect search of Dark Matter: simultaneous observation in several signal channels...

- e^+ , antiprotons, antideuteron, γ
- Measuring CR spectra up to the iron – refining propagation models;
- Solar modulation on CR spectra over 11 year solar cycle
- Direct search of primordial antimatter: Anti He, Anti C ...
- New forms of matter: strangelets
- Identification of local sources of high energy photons: SNR, Pulsars, ...

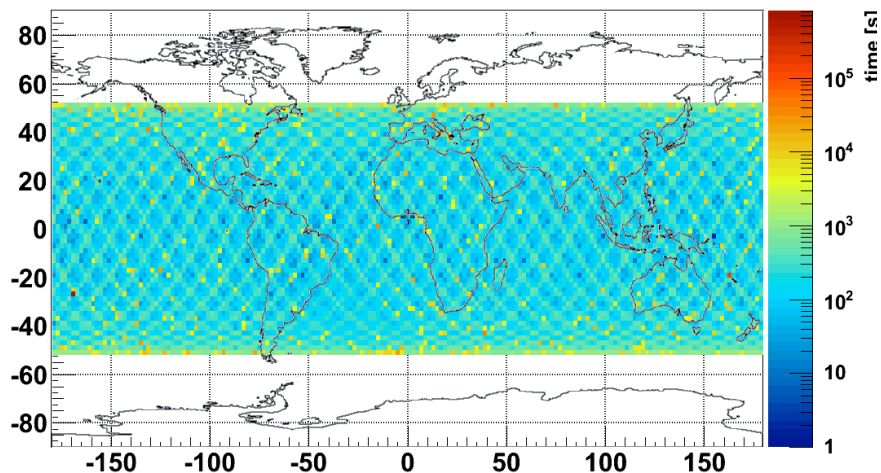


Main analysis currently on going:

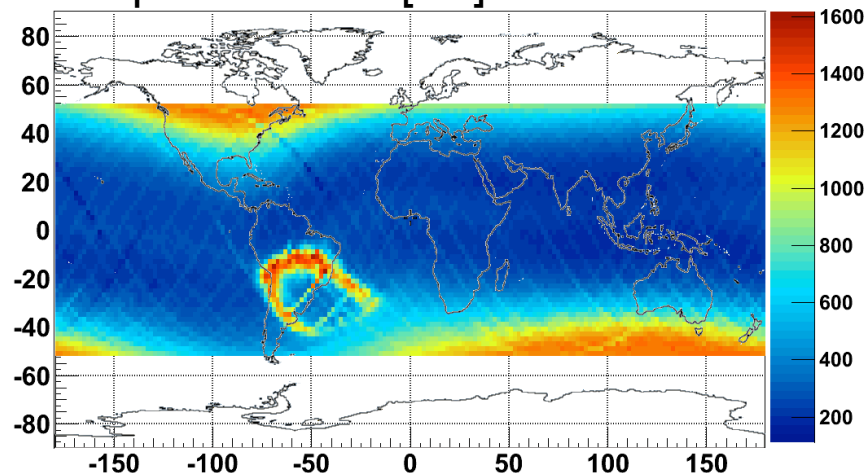
- Positron fraction
- B/C
- P, He, electron ... fluxes
- Monitor of the solar activity
- Gamma studies

AMS Orbital parameters

Time at location [s]

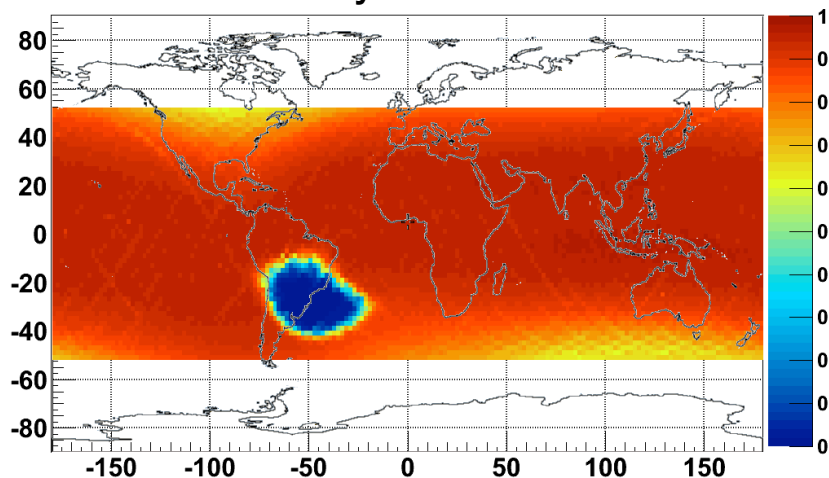


Acquisition rate [Hz]



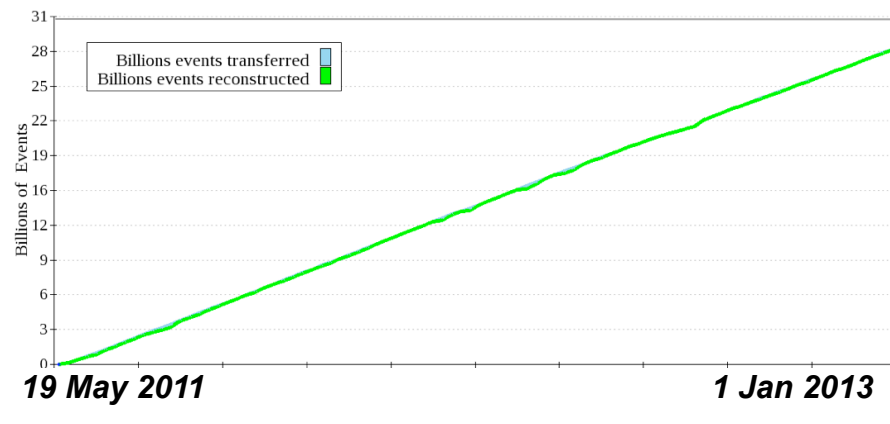
Particle rates vary from 200 to 2000 Hz per orbit

DAQ efficiency



Average DAQ efficiency 85%
Average DAQ rate ~800Hz

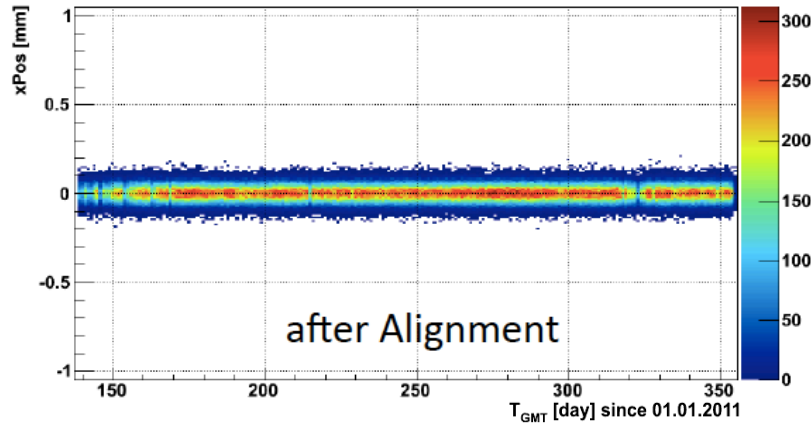
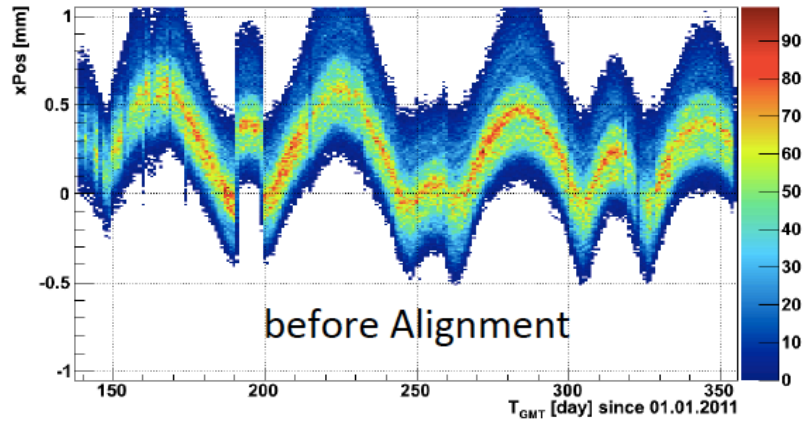
DATA collected



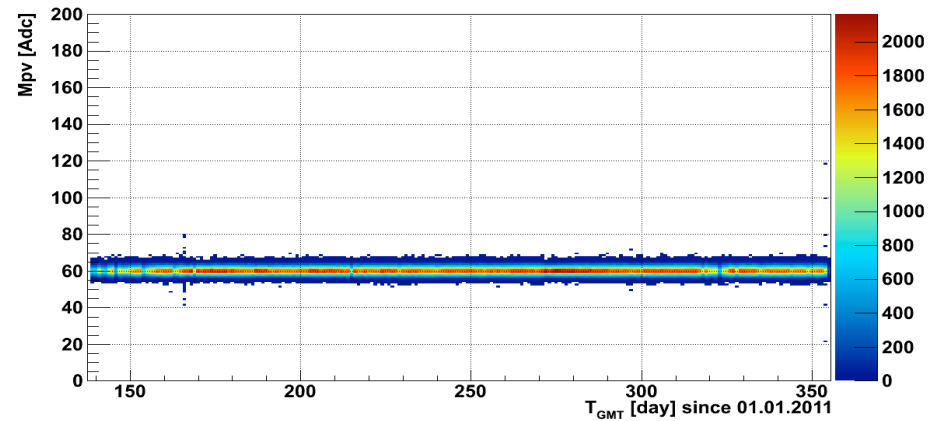
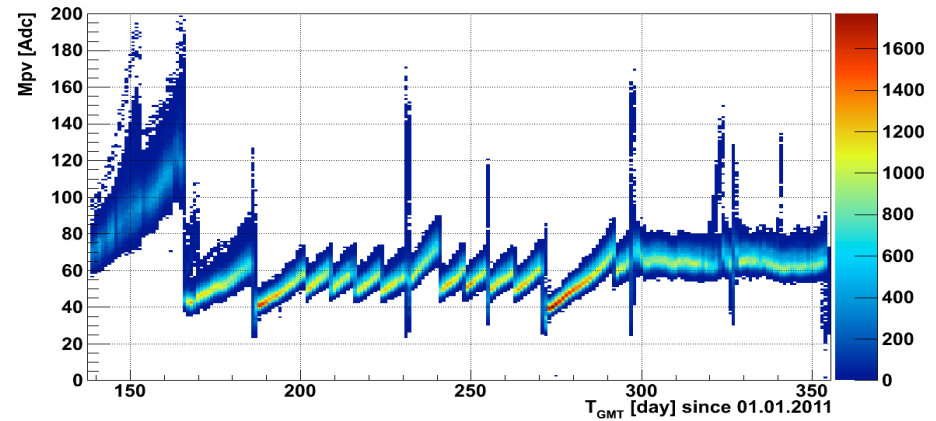
28 billion events collected in 18 months
60 TB raw events (Downlink 10 Mbit/s)

TRD offline calibration

TRD alignment

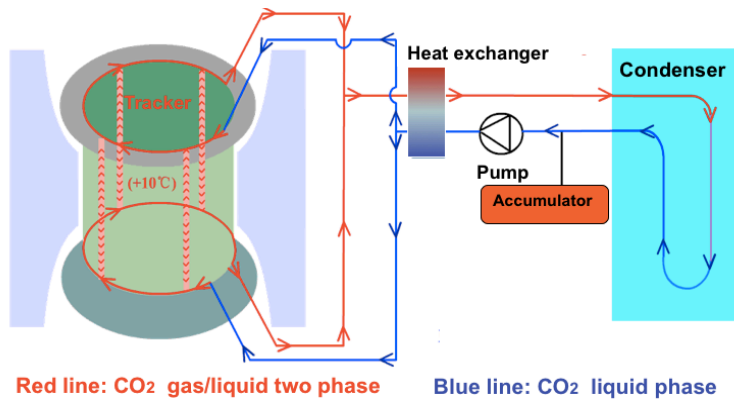


TRD gain calibration

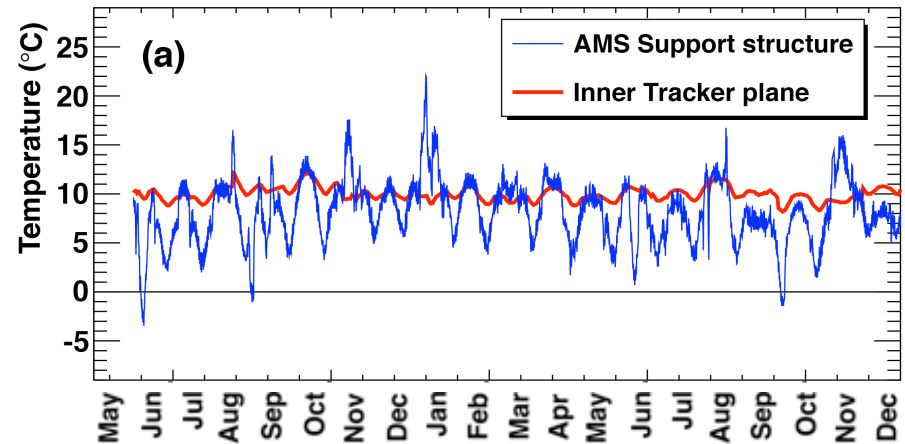


Cosmic protons are used for alignment to an accuracy of 0.04 mm for each straw module and used to calibrate the detector response to 3% accuracy.

Tracker layers thermal stability



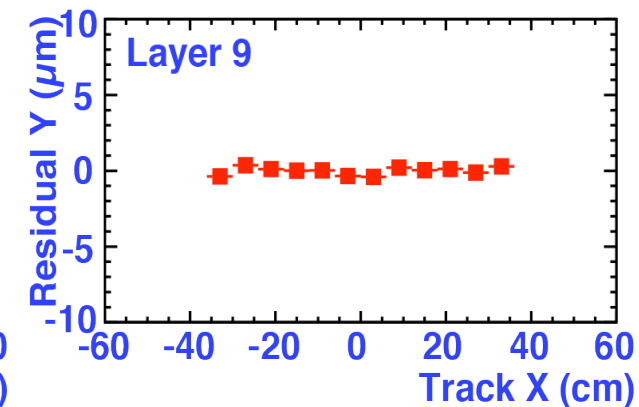
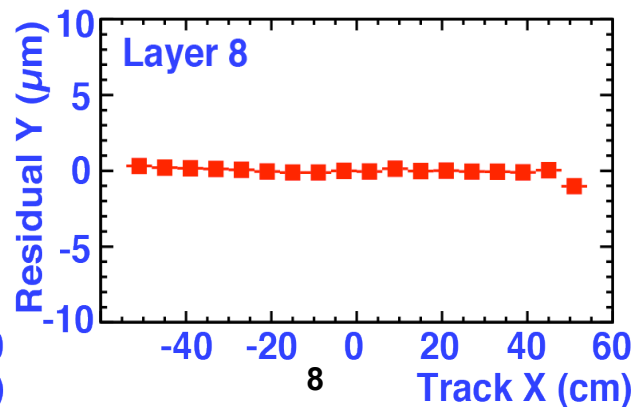
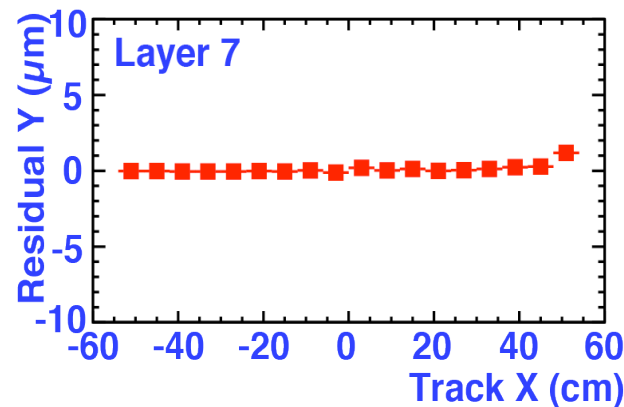
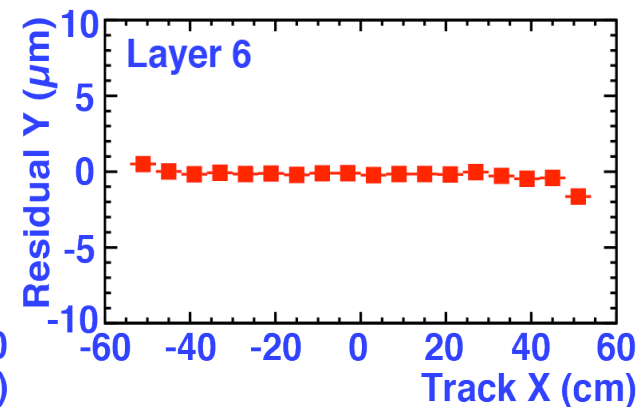
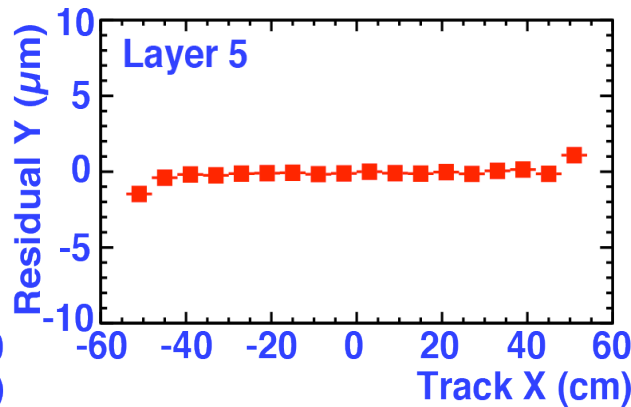
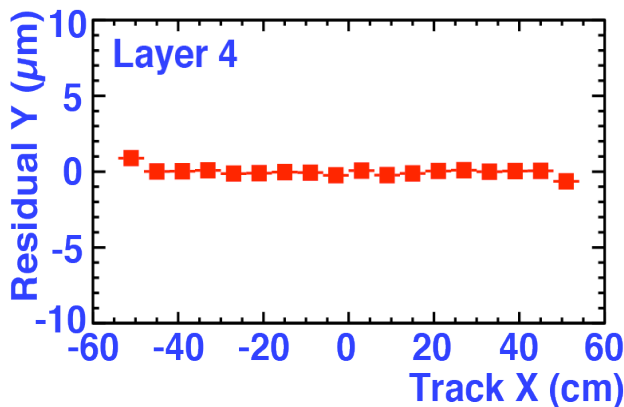
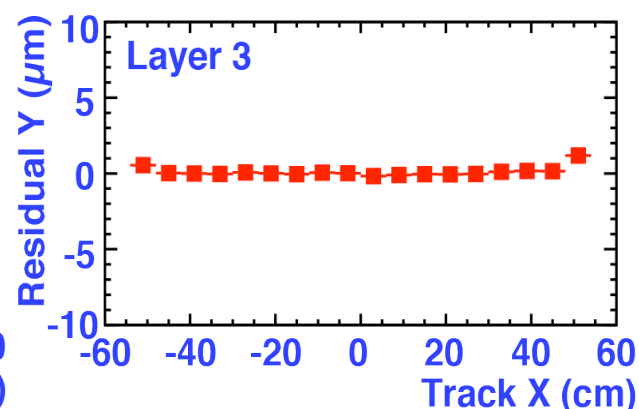
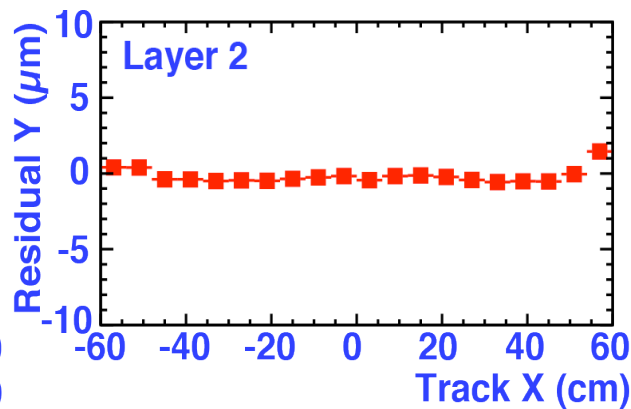
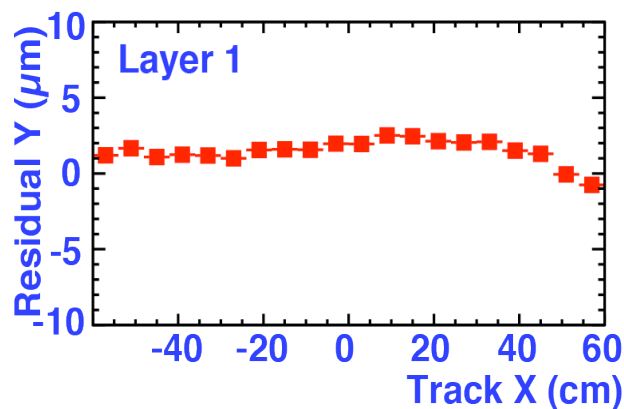
Tracker Thermal Control System



Coordinate resolution on each plane is measured with $10\ \mu\text{m}$ in the bending direction.

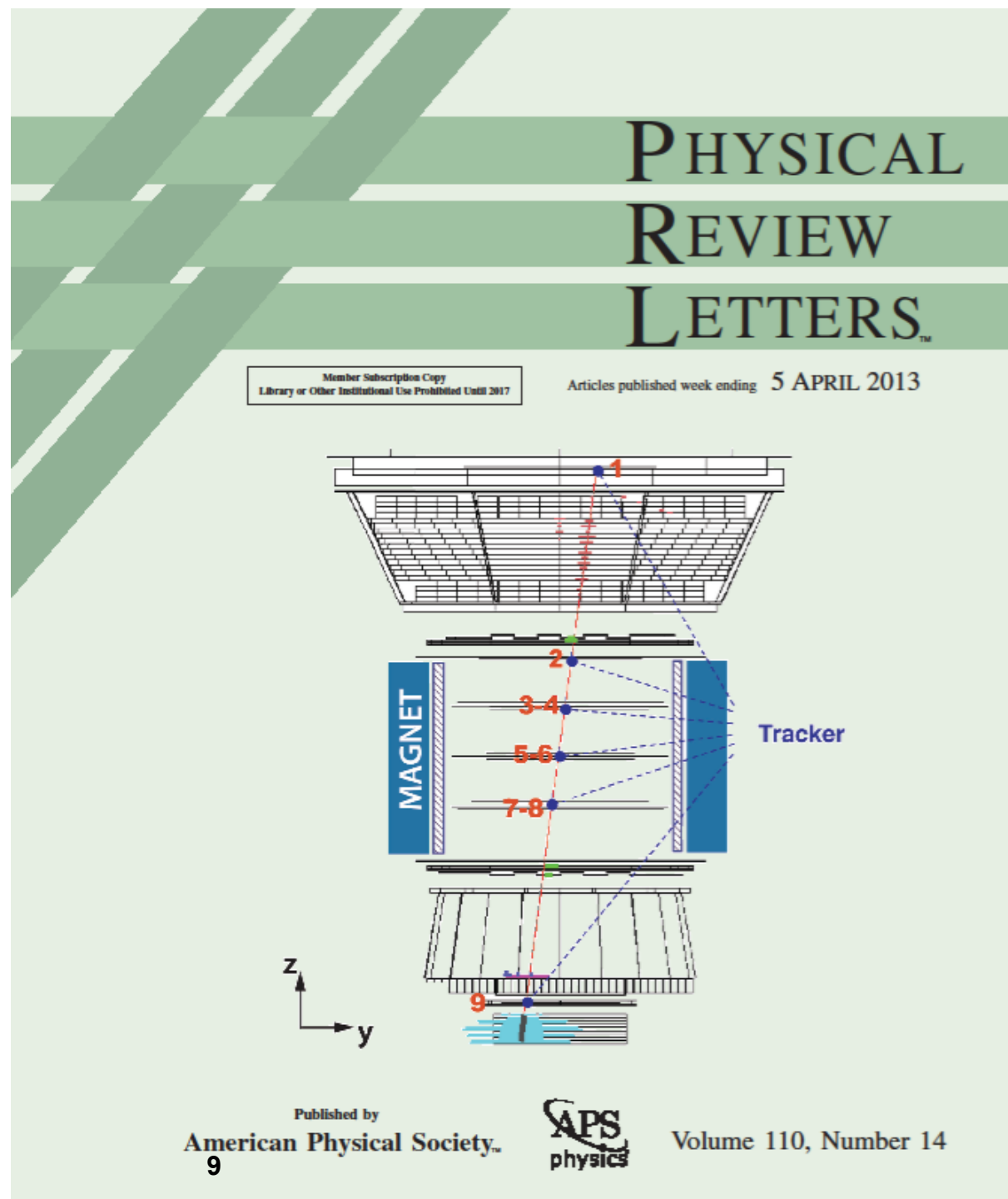
Position of ladders in the external layers are dynamically aligned to an accuracy of $3\ \mu\text{m}$.

Alignment accuracy of the 9 Tracker layers over 18 months



“First Result from the AMS on
the ISS: Precision
Measurement of the Positron
Fraction in Primary Cosmic
Rays of 0.5-350 GeV”

Selected for a
Viewpoint in Physics and
an Editors' Suggestion
[Aguilar, M. et al (AMS
Collaboration) Phys. Rev.
Lett. 110, 1411xx (2013)]



Positron identification and Proton rejection

e^+ low signal and high P background: $P \sim (10^3 \div 10^4) e^+$

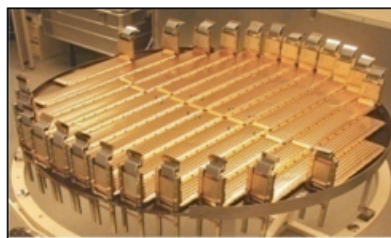
P rejection factor: $10^5 \div 10^6$ to identify e^+ with an error at % level

TRD

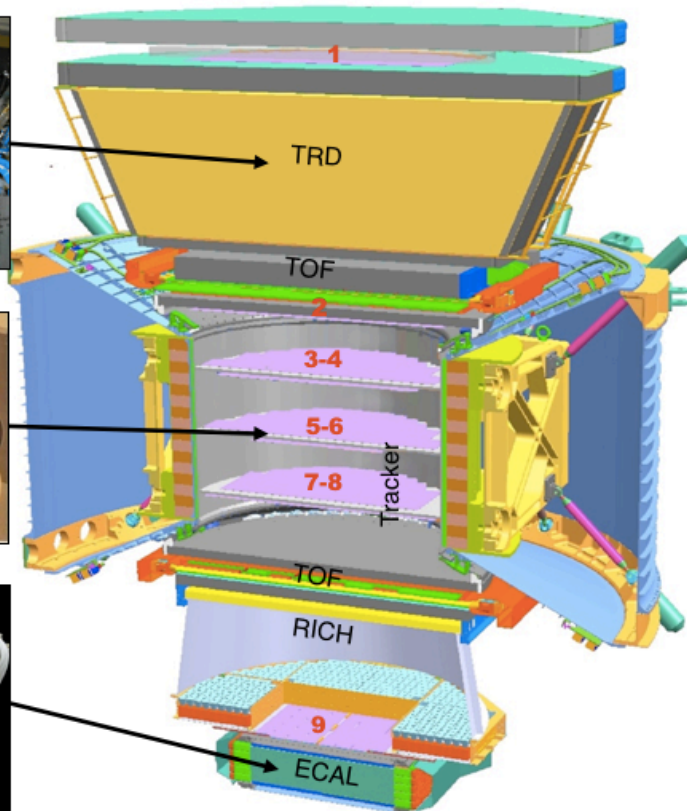
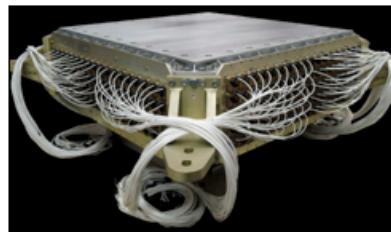
Distinguish between e^+ and P



SILICON TRACKER and MAGNET
measure the rigidity and the momentu



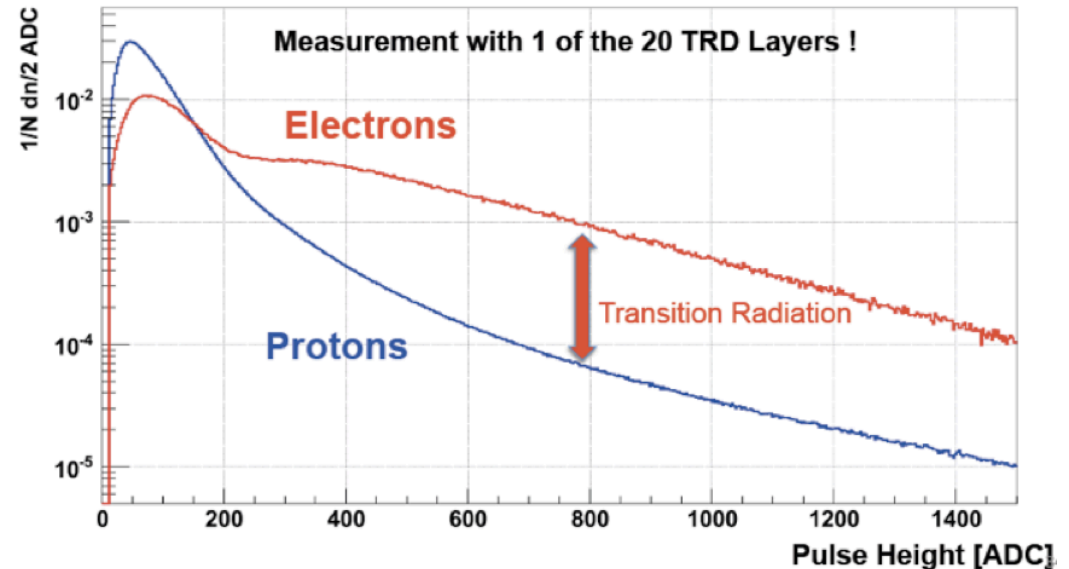
ECAL
measures the energy,
Identifies 3D characteristic positron
shower and rejects hadronic
showers



Total rejection of proton 10^6
Verified at test beam at CERN

TRD Proton rejection

Signals from 20 layers are combined in a likelihood estimator which allows an efficient discrimination of proton background

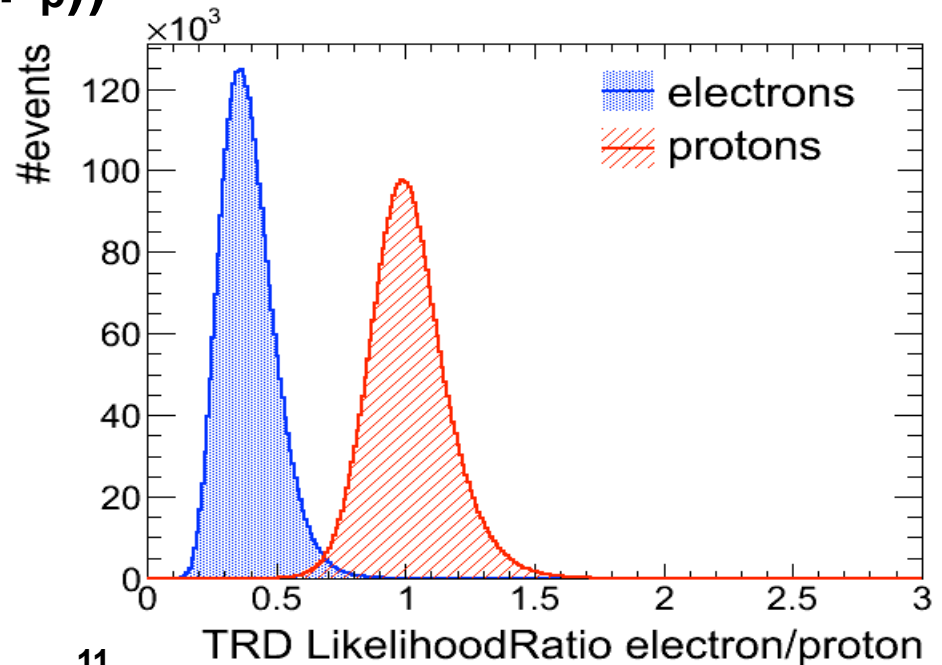


TRD estimator = $-\ln(P_e/(P_e+P_p))$

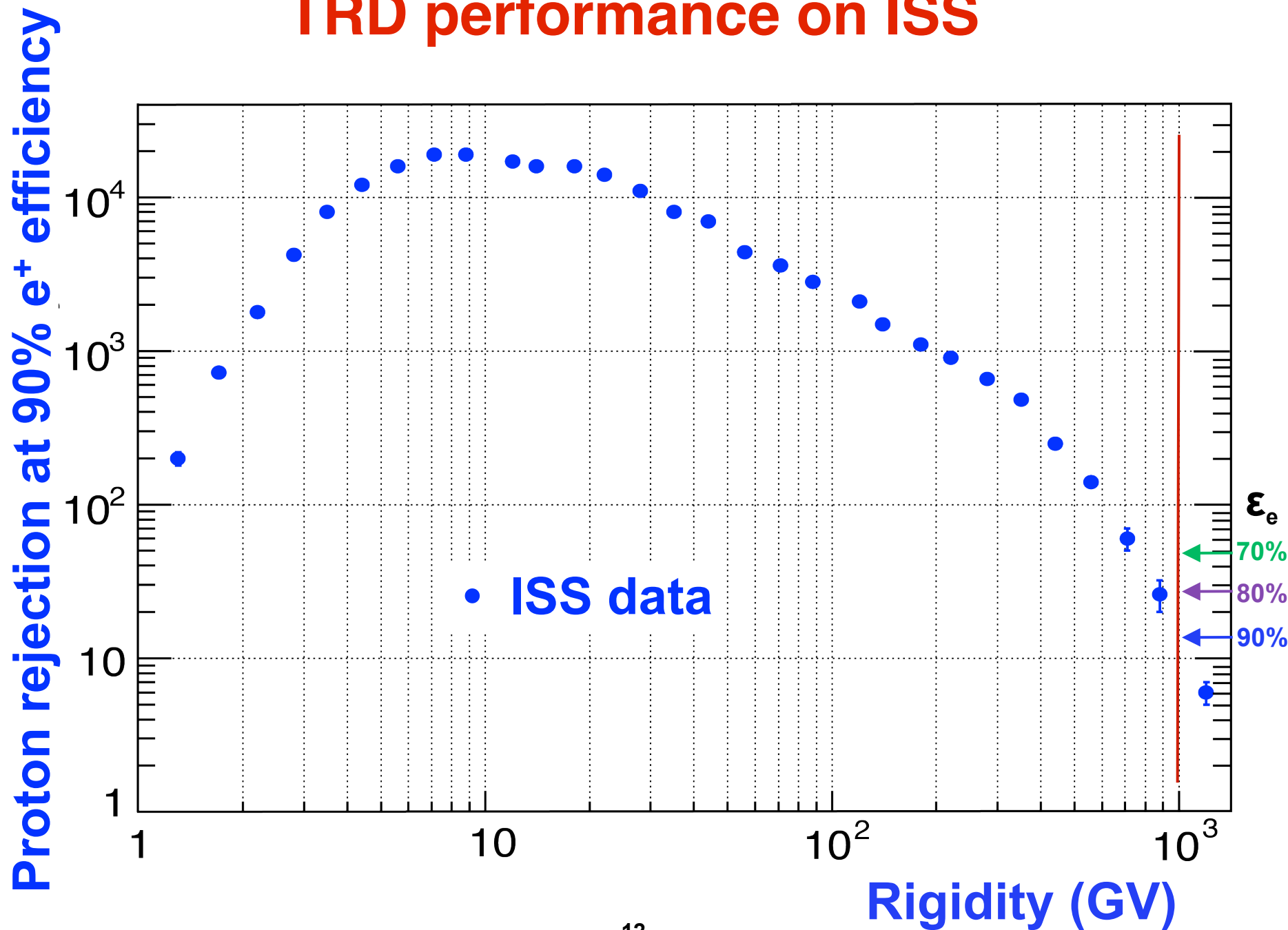
Normalized probabilities P_e and P_p

$$P_e = \sqrt[n]{\prod_i^n P_e^{(i)}(A)}$$

$$P_p = \sqrt[n]{\prod_i^n P_p^{(i)}(A)}$$



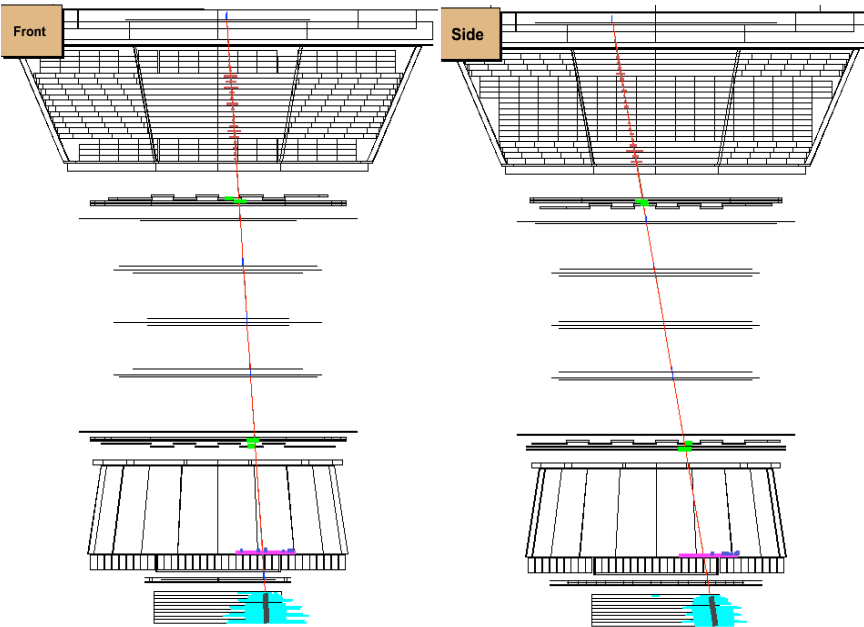
TRD performance on ISS



The Electromagnetic Calorimeter

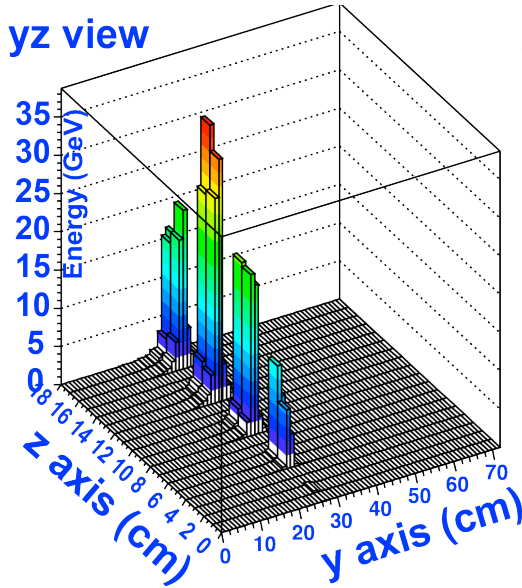
Positron $E=636$ GeV

Run/Event 133119-743/ 56950

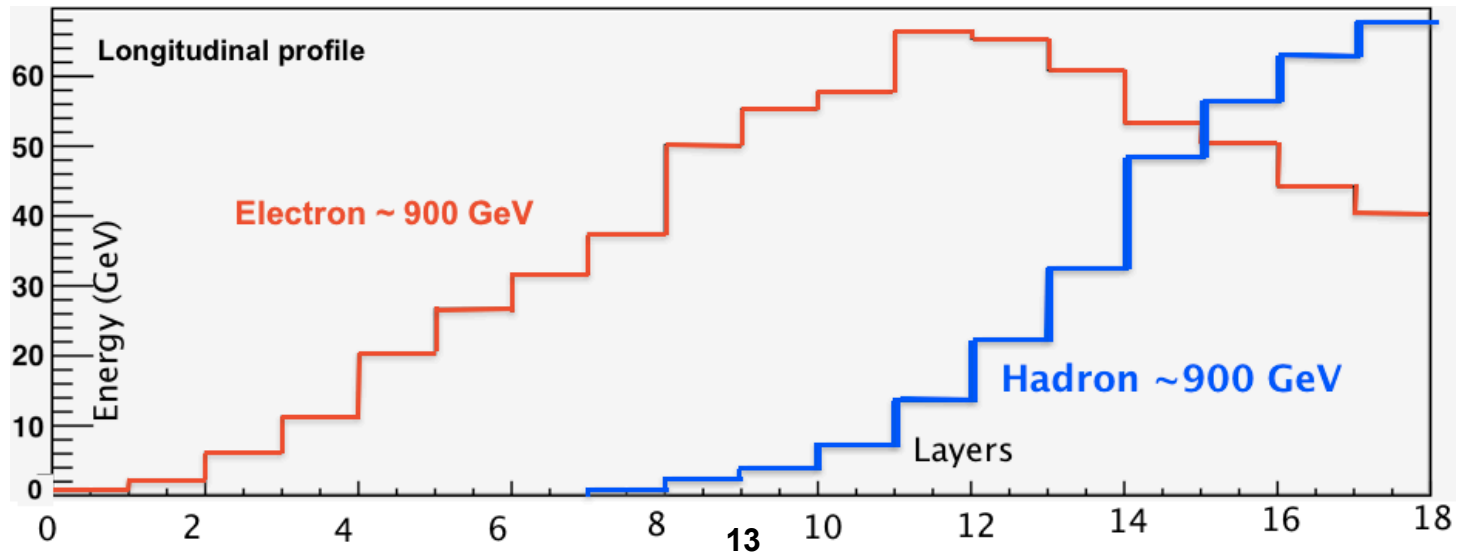
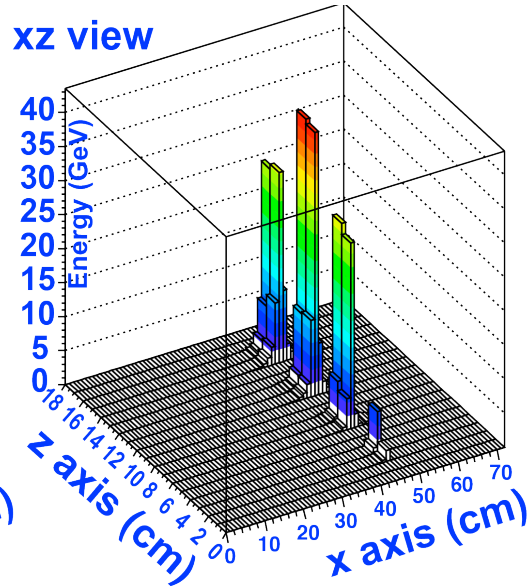


17 radiation length

yz view



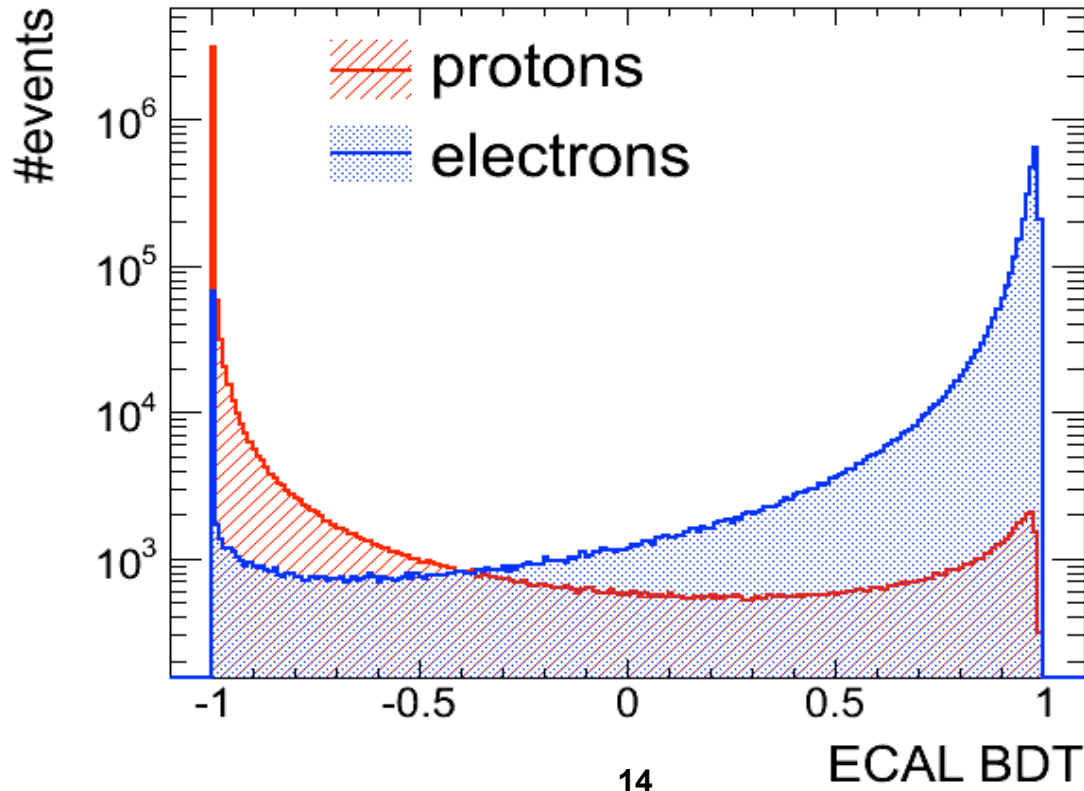
xz view



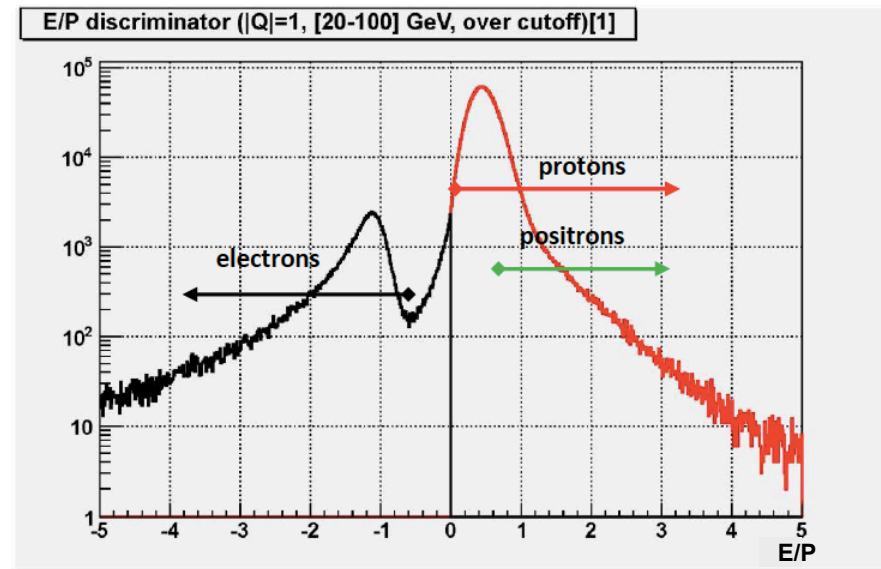
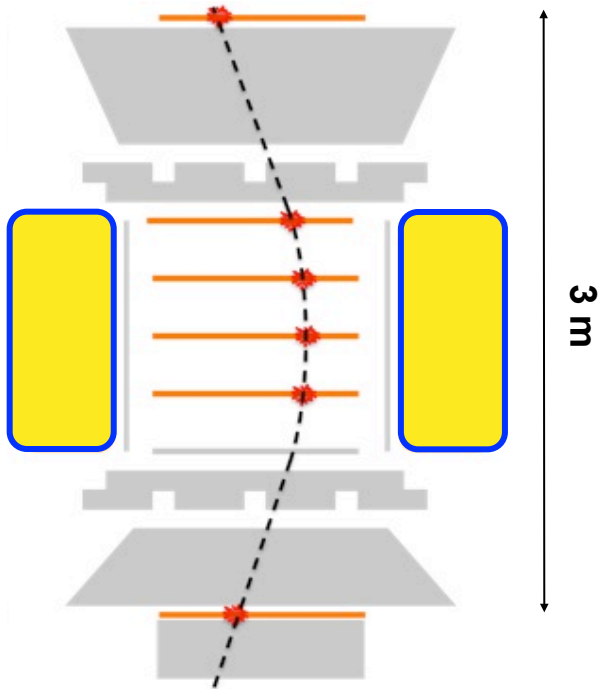
ECAL classifier

A Boosted Decision Tree (BDT) is a multivariate classifier constructed on the basis of the shower shape in the ECAL to distinguish protons and electrons.

The BDT exploits non linear correlation among variables to separate two different populations.



Tracker e+ and e- identification and P rejection

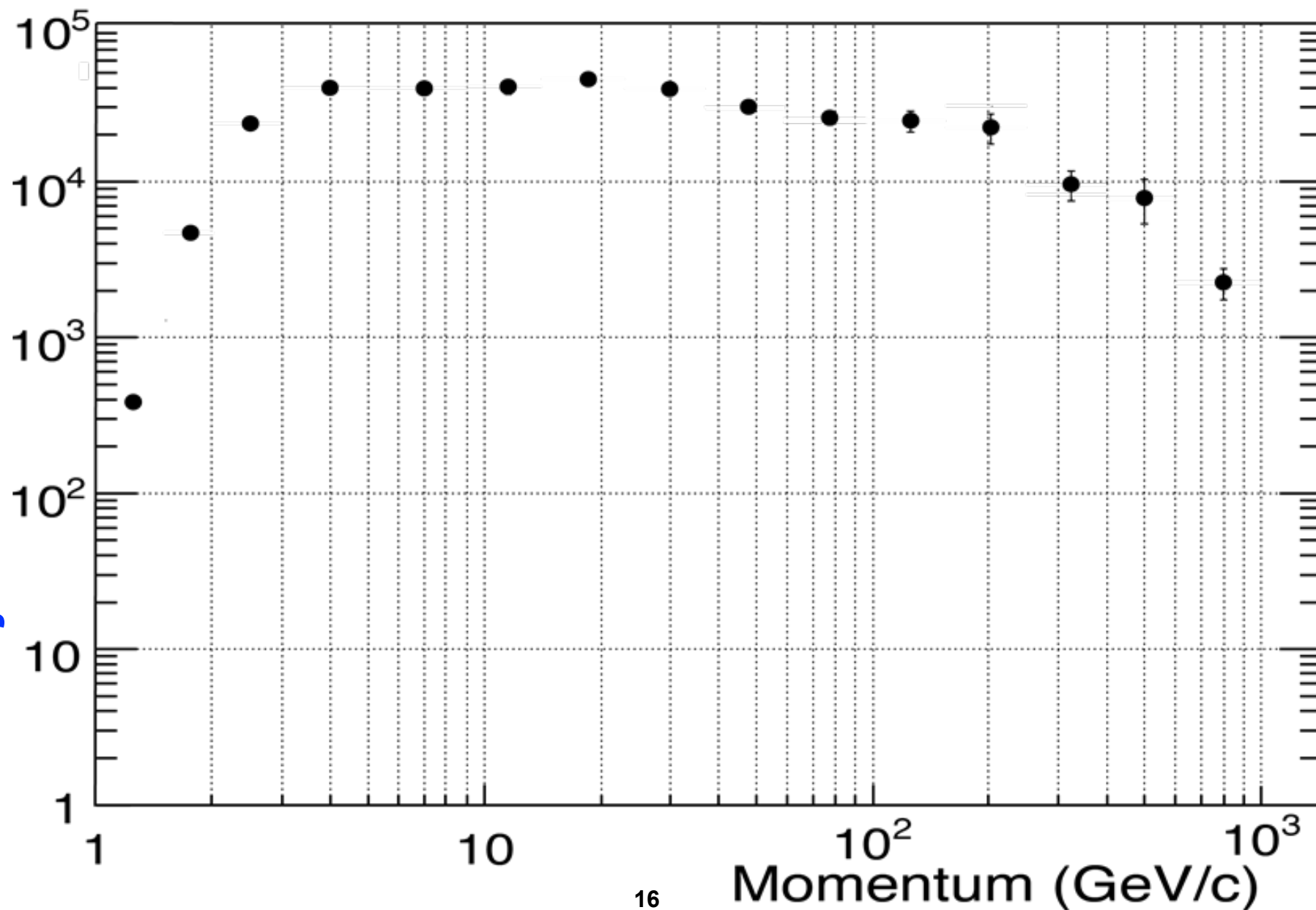


A fit of particle trajectory is used to measure the sign of the particle and its momentum P :

- 1) Used to suppress e^-
- 2) compared to the energy E measured by ECAL, E/P is used to suppress Protons

Proton rejection using ECAL and E/P

Proton rejection at 90% e^+ efficiency



Data Selection

- Dataset: 19 May 2011-10 December 2012, 18 months
- More than 25 billion of events
- Energy range: 0.5 – 350 GeV
- No SAA
- Down going particle
- Energy > Geomatic Cut Off
- ECAL Fiducial volume
- Track – Shower position matching

Analysis Steps

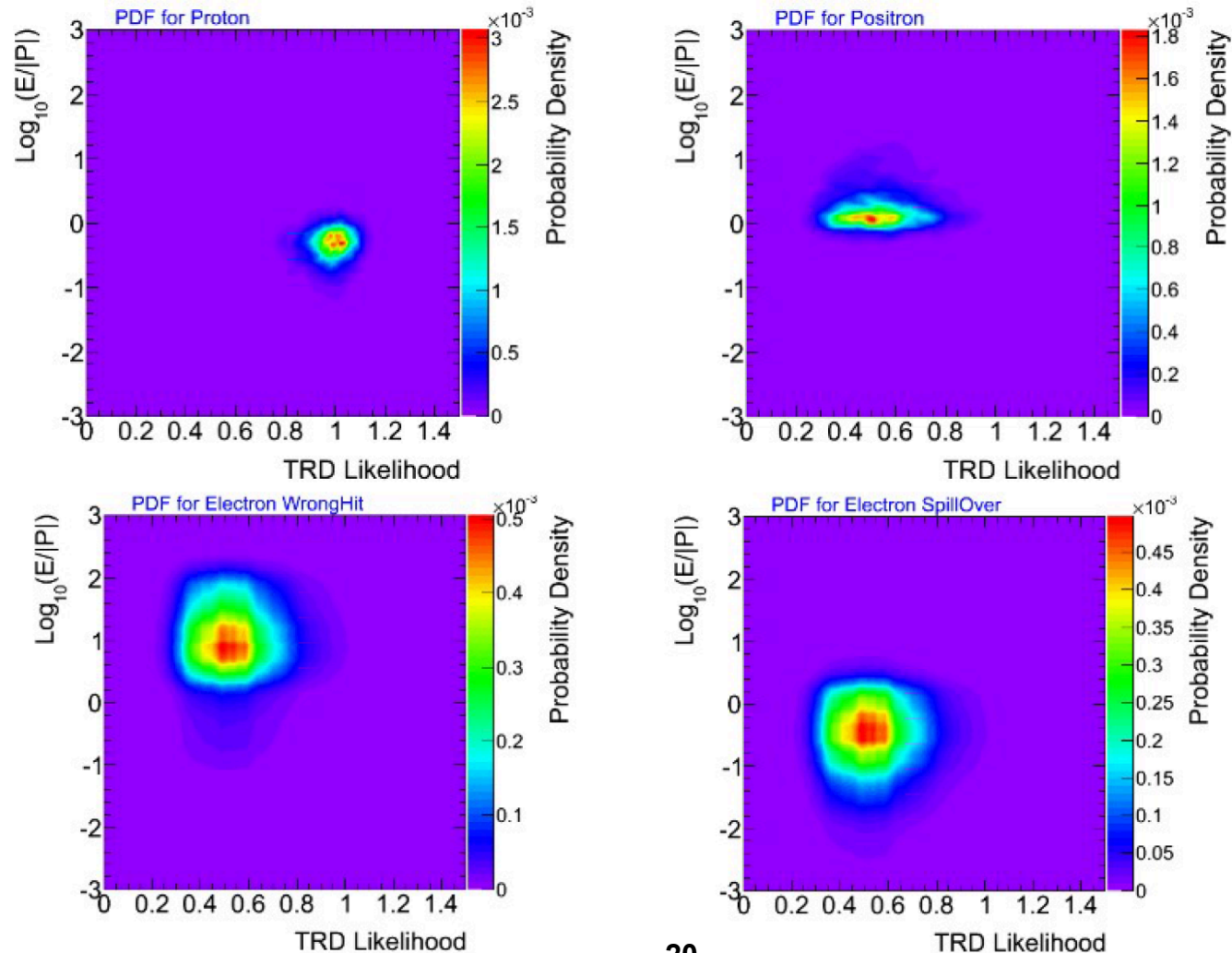
- Remove proton background with cuts on ECAL classifiers
- Study of the charge confusion: the probability of misidentify the sign of the charge (background due to e^-)
- Build 2D templates: signal (electrons) and background (protons) from Data, charge confused signal from MC
- Fit TRD likelihood vs EoP with templates, extracting: N_{ele} , N_{pos} , N_{pro} , N_{cc} from N_{ele}
- Evaluation of the systematic error

Study of the charge confusion

- TB and MC have been used to define the shapes of the different charge confusion contributions
- Two sources of charge confusion for electrons/positrons on TB:
 - Spill over (due to resolution effect)
 - Wrong hits (due to scattering, interactions, backscattering)
- Relative contribution of the two sources changes with energy
- Different methods have been studied giving compatible results

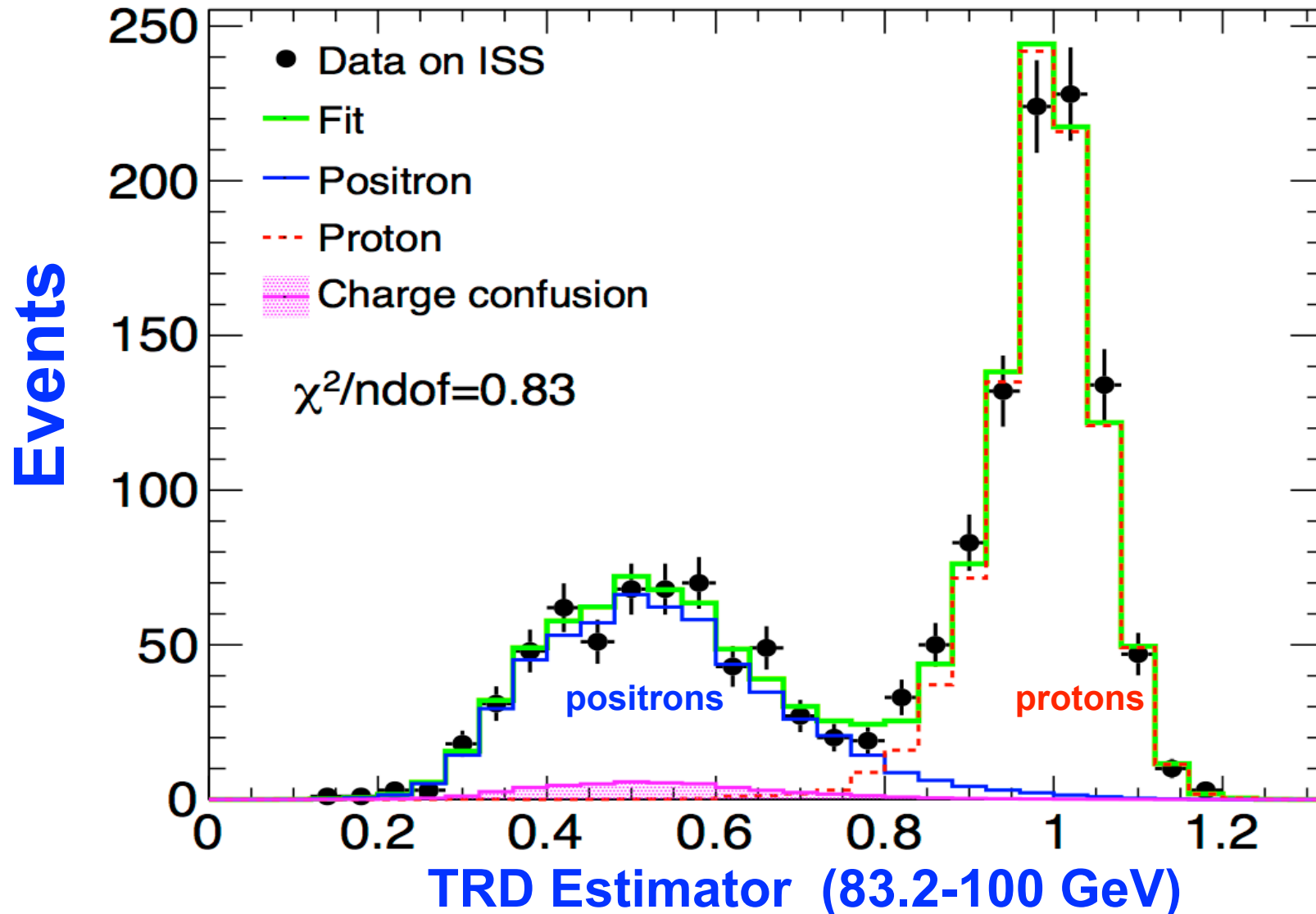
Analysis steps: 2D templates fitting

Nearly 6.8 million of primary electrons and positrons



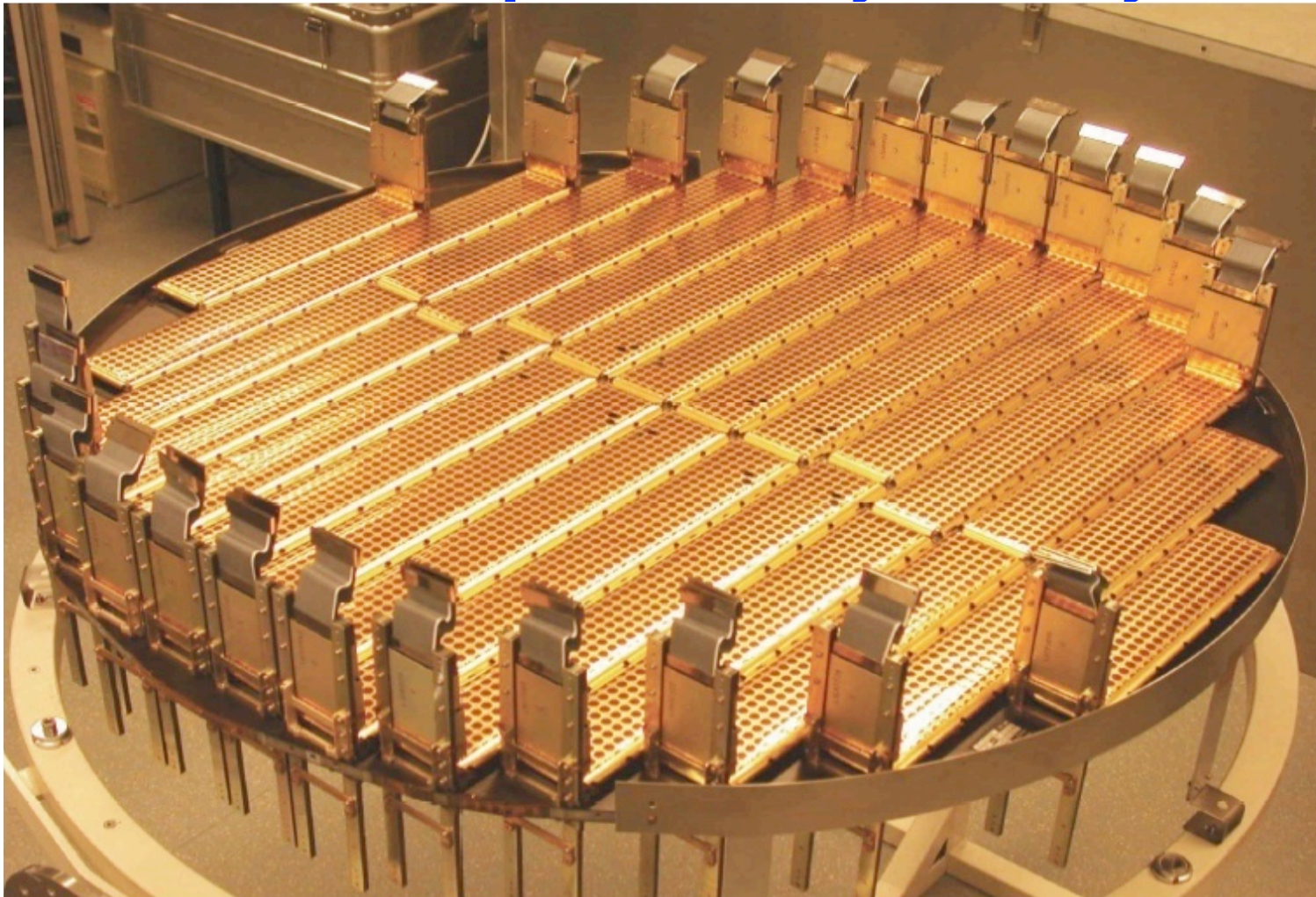
2D FIT results projected on the TRD estimator

Fit TRD e/p likelihood vs EoP with templates, extracting: Nele, Npos, Npro, Ncc



Systematic error on the positron fraction:

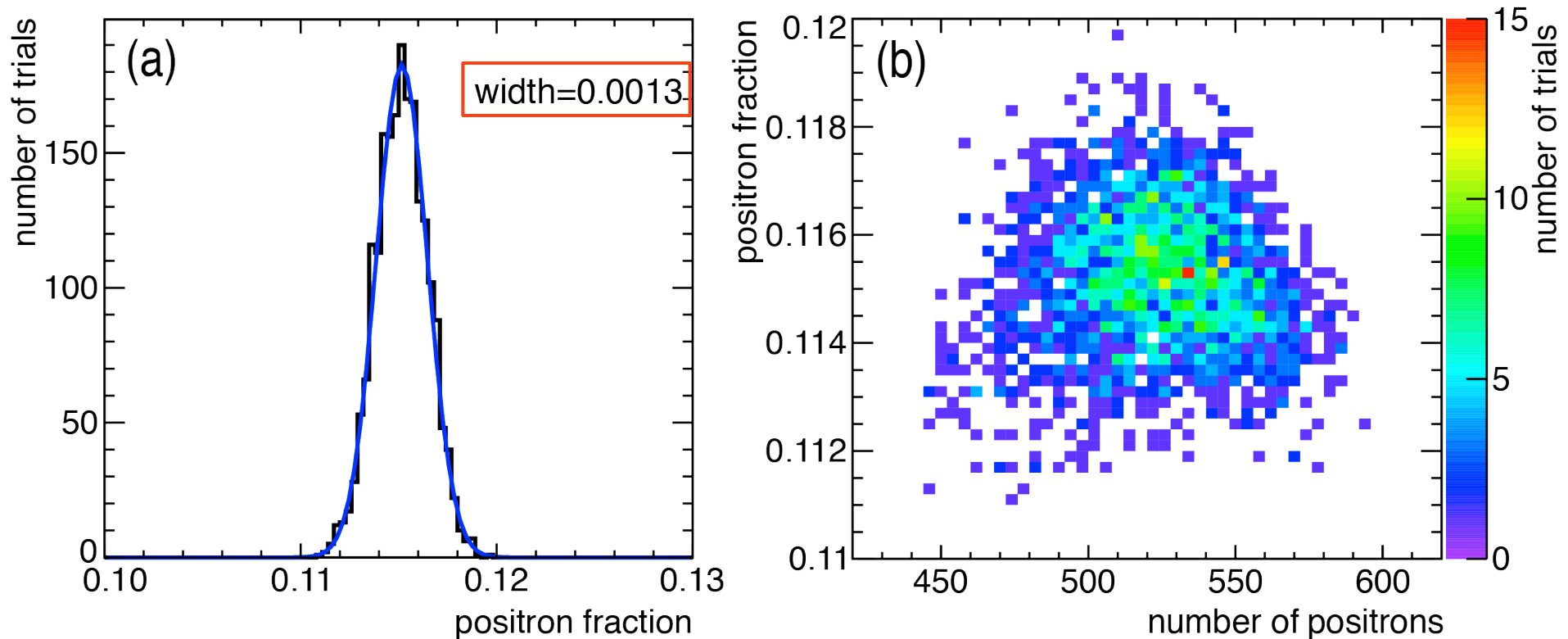
1. acceptance asymmetry



Difference between positron and electron acceptance due to known minute tracker asymmetry

Systematic error on the positron fraction:

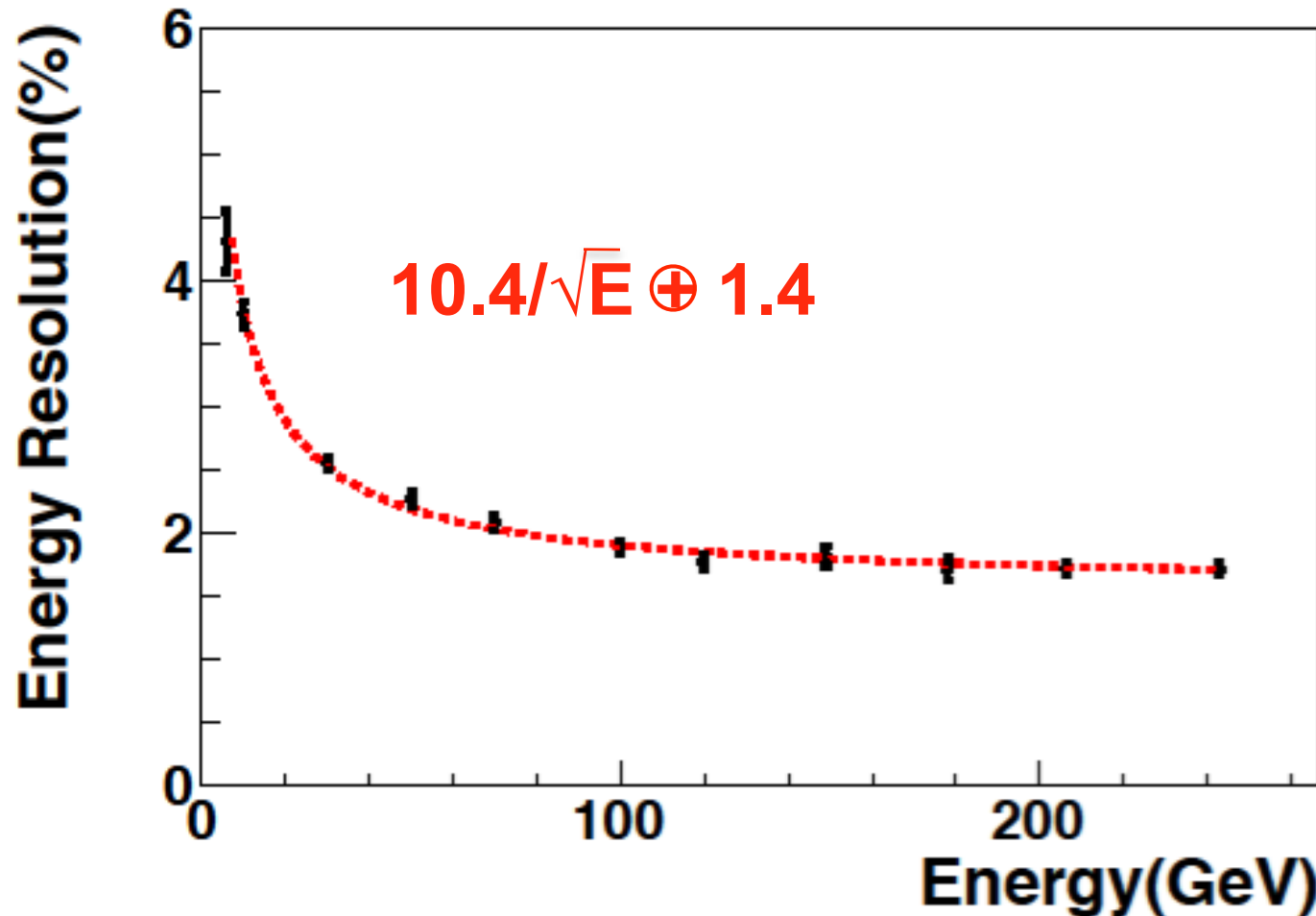
2. Selection dependence



For each energy bin, over 1,000 sets of cuts were analyzed.
No correlation between number of positron and positron fraction.
The measurement is stable over wide variations of the cuts
in the TRD identification, ECAL Shower Shape,
E (from ECAL) matched to IPI (from the Tracker).

Systematic error on the positron fraction:

3. Bin-to-bin migration

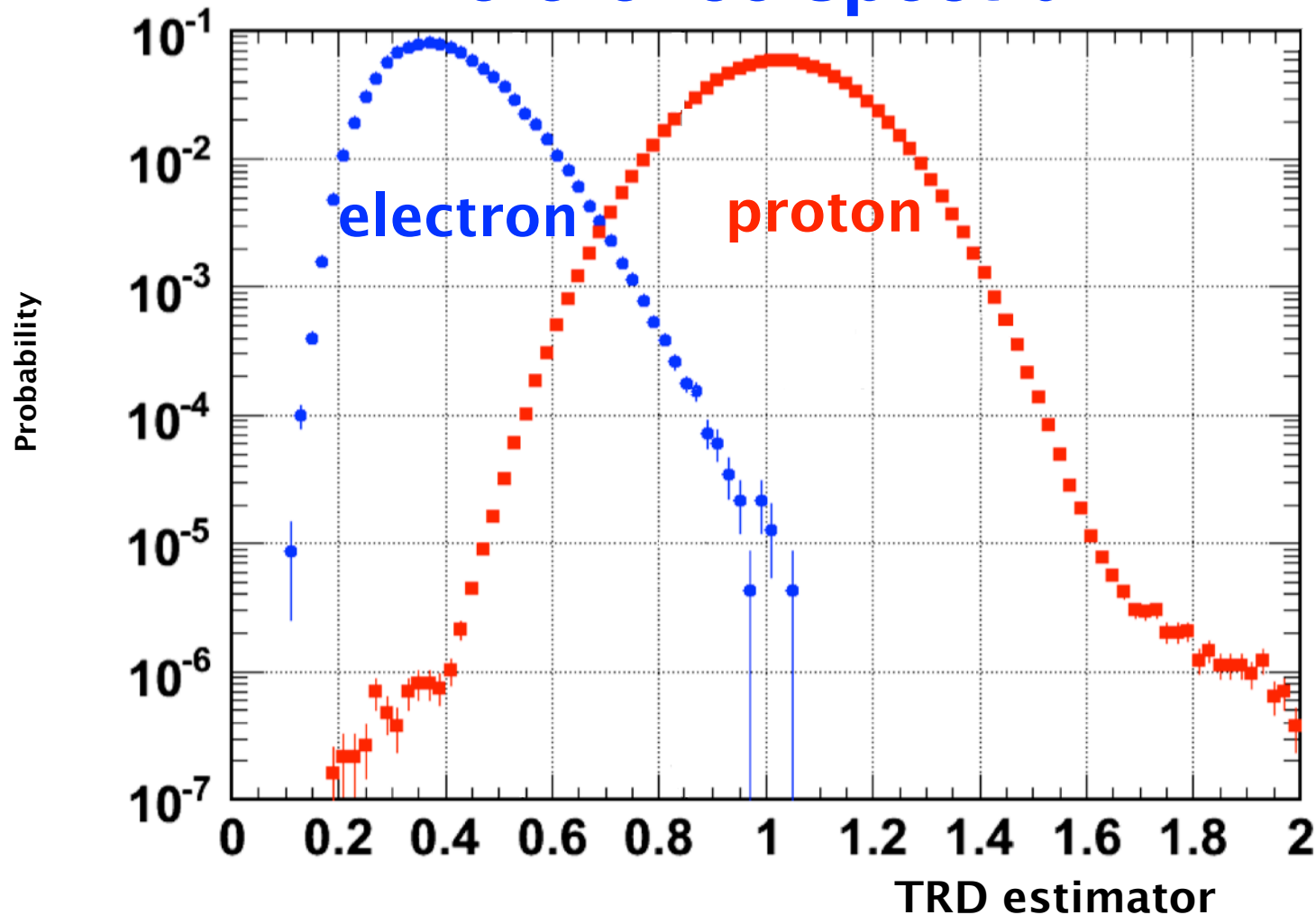


Event migration effects are obtained by folding the measured spectra of positrons and electrons with the ECAL energy resolution.

Bin width: 2σ up to 5 GeV; 4σ up to 50 GeV; 8σ up to 100 GeV; 19σ up to 300 GeV.

Systematic error on the positron fraction:

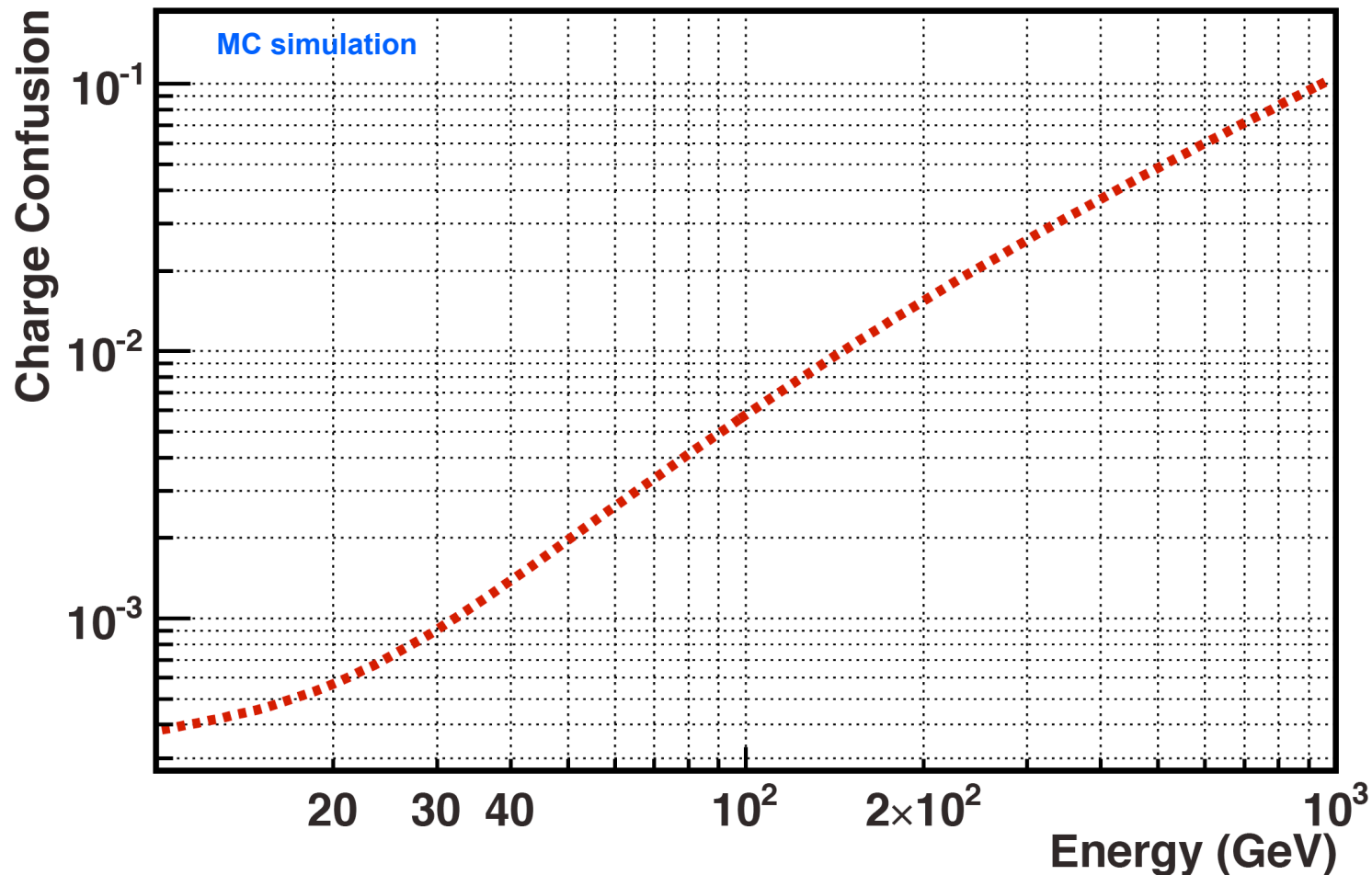
4. Reference spectra



Definition of the reference spectra is based on pure samples of electrons and protons of finite statistics.

Systematic error on the positron fraction:

5. Charge confusion



Systematic errors correspond to variations of these effects within their statistical limits.

Difference between Data and MC added to systematic error

Systematic errors to positron fraction

1. Acceptance asymmetry

- Difference between positron and electron acceptance due to known minute tracker asymmetry

2. Selection dependence

- Dependence of the result on the cut values

3. Migration bin-to bin

- Migration of electron and positron events from the neighboring bins affects the measured fraction

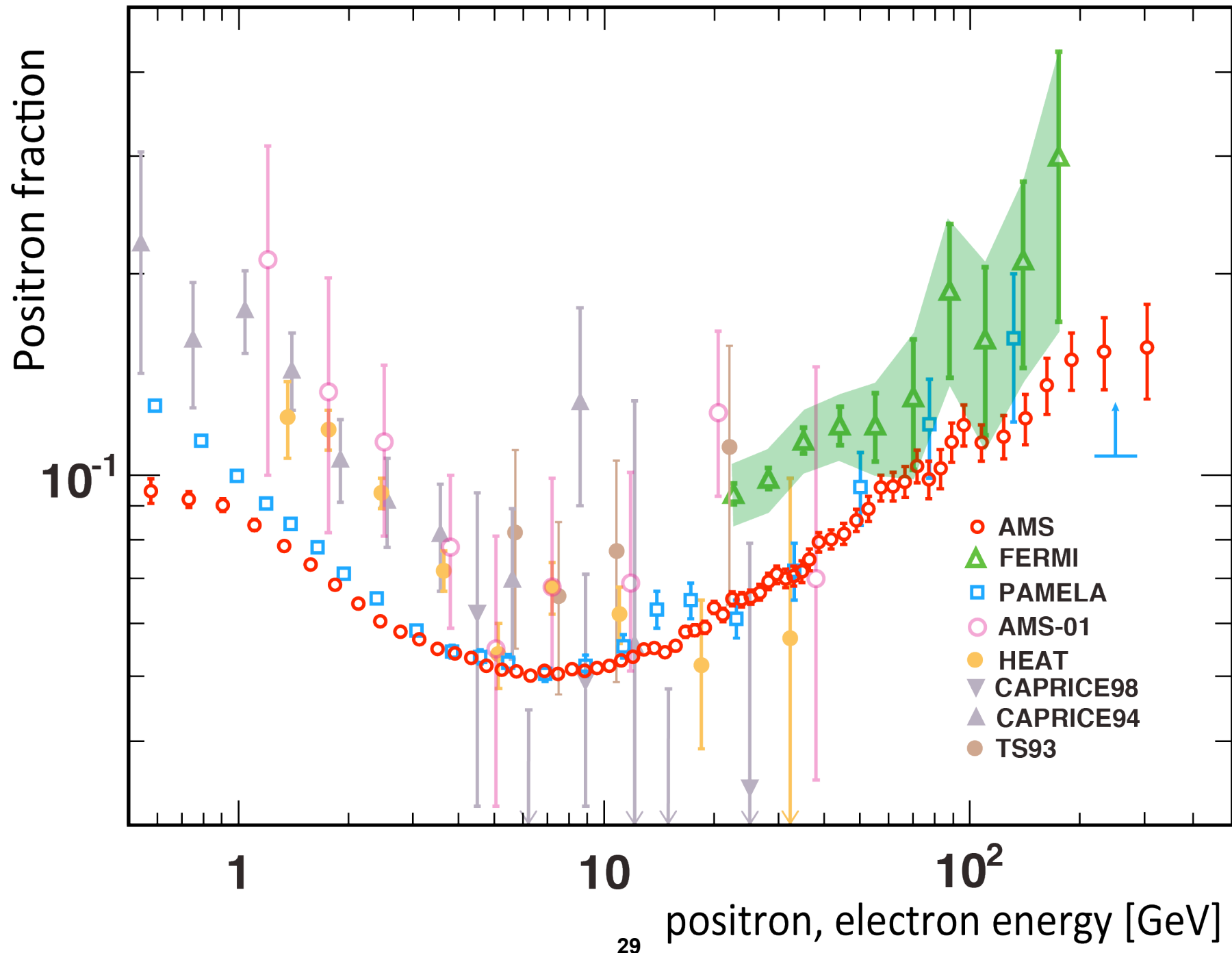
4. Reference spectrum

- Definition of the reference spectra is based on pure samples of electrons and protons of finite statistics

5. Charge confusion

- Two sources: large angle scattering and production of secondary tracks along the path of the primary track. Both are well reproduced by MC. Systematic errors correspond to variations of these effects within their statistical limits.

Energy[GeV]	N _{e+}	Fraction	$\sigma_{stat.}$	$\sigma_{acc.}$	$\sigma_{sel.}$	$\sigma_{mig.}$	$\sigma_{ref.}$	$\sigma_{c.c.}$	$\sigma_{syst.}$
59.36 - 64.03	448	0.0962	0.0047	0.0002	0.0009	0.0000	0.0002	0.0006	0.0011
64.03 - 69.00	392	0.0978	0.0050	0.0002	0.0010	0.0000	0.0002	0.0007	0.0013
69.00 - 74.30	324	0.1032	0.0057	0.0002	0.0010	0.0000	0.0002	0.0009	0.0014
74.30 - 80.00	276	0.0985	0.0062	0.0002	0.0010	0.0000	0.0002	0.0010	0.0014
80.00 - 86.00	232	0.1023	0.0067	0.0002	0.0010	0.0000	0.0002	0.0010	0.0014
86.00 - 92.50	240	0.1120	0.0075	0.0002	0.0010	0.0000	0.0003	0.0011	0.0015
92.50 - 100.0	226	0.1189	0.0081	0.0002	0.0011	0.0000	0.0003	0.0012	0.0017
100.0 - 115.1	304	0.1118	0.0066	0.0002	0.0015	0.0000	0.0003	0.0015	0.0022
115.1 - 132.1	223	0.1142	0.0080	0.0002	0.0019	0.0000	0.0004	0.0019	0.0027
132.1 - 151.5	156	0.1215	0.0100	0.0002	0.0021	0.0000	0.0005	0.0024	0.0032
151.5 - 173.5	144	0.1364	0.0121	0.0002	0.0026	0.0000	0.0006	0.0045	0.0052
173.5 - 206.0	134	0.1485	0.0133	0.0002	0.0031	0.0000	0.0009	0.0050	0.0060
206.0 - 260.0	101	0.1530	0.0160	0.0003	0.0031	0.0000	0.0013	0.0095	0.0101
260.0 - 350.0	72	0.1550	0.0200	0.0003	0.0056	0.0000	0.0018	0.0140	0.0152



Comparing AMS data with a minimal model

Sum of diffuse power law spectra and a single common source of e^\pm

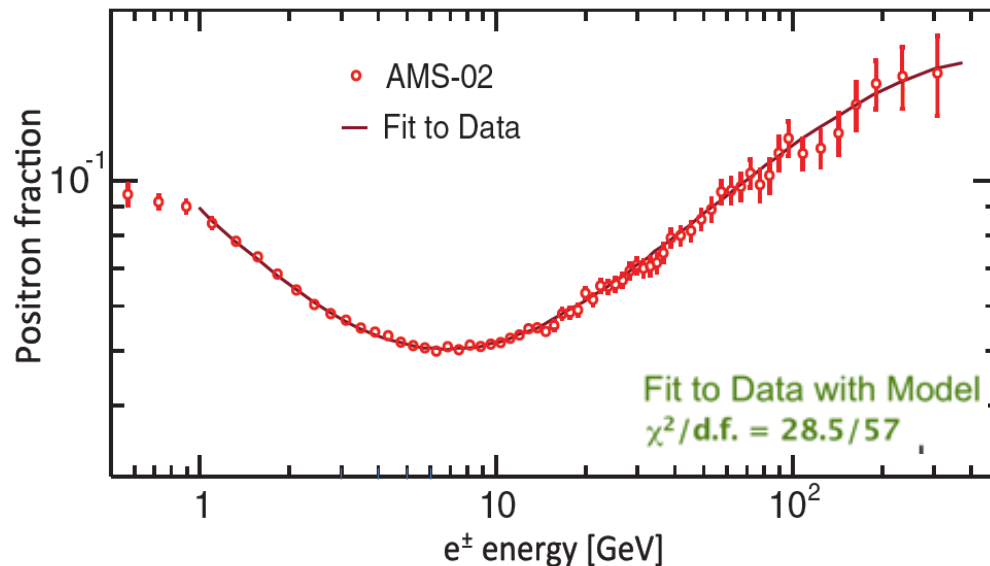
- $\Phi_{e^+} = C_{e^+} E^{-\gamma_{e^+}} + C_s E^{-\gamma_s} e^{-E/E_s}$ (C_{e^+} C_{e^-} C_s relative weights)
- $\Phi_{e^-} = C_{e^-} E^{-\gamma_{e^-}} + C_s E^{-\gamma_s} e^{-E/E_s}$ (E_s : cutoff energy for the source spectrum)

$\gamma_{e^-} - \gamma_{e^+} = -0.63 \pm 0.03$ the diffuse e^+ is **softer** than the diffuse e^-

$\gamma_{e^-} - \gamma_s = 0.66 \pm 0.05$ the source is **harder** than the diffuse e^-

$C_{e^+}/C_{e^-} = 0.091 \pm 0.001$ the diffuse e^+ amounts to ~10% of the diffuse e^-

$C_s/C_{e^-} = 0.0078 \pm 0.0012$ the source constitutes ~1% of the diffuse e^-



$1/E_s = 0.0013 \pm 0.0007 \text{ GeV}^{-1}$
corresponding to a cutoff energy
of $760^{+1000}_{-280} \text{ GeV}$.

The positron fraction spectrum is consistent with e^\pm fluxes given by the sum of the diffuse spectrum and a single common power law source.

Study of the Anisotropy

The source of e^\pm may induce some degree of anisotropy of the measured positron to electron ratio.

The fluctuations are described using the spherical harmonic expansion

$$\frac{r_e(b, l)}{\langle r_e \rangle} - 1 = \sum_{\ell=0}^{\infty} \sum_{m=-\ell}^{\ell} a_{\ell m} Y_{\ell m}(\pi/2 - b, l)$$

$r_e(b, l)$ denotes the positron fraction at (b, l) , $\langle r_e \rangle$ is the average ratio, $Y_{\ell m}$ are the spherical harmonic function and $a_{\ell m}$ are the corresponding weights.

The coefficients of the angular power spectrum are defined as

$$C_\ell = \frac{1}{2\ell + 1} \sum_{m=-\ell}^{\ell} |a_{\ell m}|^2.$$

consistent with isotropy at all energies

Limits on the amplitude of a dipole anisotropy in any axis in galactic coordinates on the positron to electron ratio

$$\delta = 3\sqrt{C_1/4\pi} \leq 0.036 \quad (95\% \text{ C.L.})$$

Conclusion

The first 6.8 million primary e^+ and e^- events collected with AMS on the ISS show:

- i. At energies < 10 GeV, a decrease in the positron fraction with increasing energy.
- ii. A steady increase in the positron fraction from 10 to ~ 250 GeV.
- iii. The determination of the behavior of the positron fraction from 250 to 350 GeV and beyond requires more statistics.
- iv. The slope of the positron fraction versus energy decreases by an order of magnitude from 20 to 250 GeV and no fine structure is observed. The agreement between the data and the model shows that the positron fraction spectrum is consistent with e^\pm fluxes each of which is the sum of its diffuse spectrum and a single common power law source.
- v. The positron to electron ratio is consistent with isotropy; $\delta \leq 0.036$ at the 95% C.L.

These observations confirm the existence of new physical phenomena, whether from a particle physics or an astrophysical origin.



More science coming soon! Stay tuned!!!